COMPARISON OF WHITE-BOX AND BLACK-BOX MODELS OF A REAL HYDRAULIC PUMPING SYSTEM USING A VARIABLE SPEED DRIVE

Erlon Cavazzana
Bruno Henrique Barbosa
Leonardo Antônio Borges Tôrres
Carlos Barreira Martinez

erlon,brunohb,torres@cpdee.ufmg.br
martinez@cce.ufmg.br

Universidade Federal de Minas Gerais, Belo Horizonte, Brazil
CPH - Centro de Pesquisas Hidráulicas e Recursos Hídricos

Abstract. *This paper presents black-box and white-box models of a real hydraulic pumping system. The aim is to build models that explain the dynamic and static behavior of a hydraulic engineering test bench from real data. Firstly, a neural NARMAX black-box model was obtained. Secondly, a white-box model was developed subdividing the test bench into four subsystems: induction motor and inverter drive; centrifugal pump; fixed hydraulic subsystem; and variable hydraulic load. Using a variable frequency drive as the final control element, dynamic tests were conducted to validate the models in various operating points. A comparison of the proposed approaches based on the models performance evaluation is presented.*

Keywords: *centrifugal pumps, variable speed pumping, white-box model, black-box model, neural NARMAX.*

1 INTRODUCTION

In the last years, the power electronics and electrical drives control techniques evolution allowed the Variable Frequency Drivers (VFDs) to become commom equipments in the industry.

The use of VFDs in pumping systems is of great interest (Irvine and Gibson, 2002) due to the benefits provided by the variable speed pumping approach (Pemberton, 2005), such as: energy saving (Carlson, 2000), hydraulic system soft operation, and therefore lower maintenance needs (Guevara and Carmona, 1990). Moreover this control strategy seems to be more effective than other alternatives (Driedger, 1995). In this context, accurate modelling of variable speed pumping systems is essential to design high efficiency control algorithms.

The objective of the present work is to obtain and to compare the performance of static and dynamic models for a hydraulic test bench that uses VFDs. This modelling is pursued in order to further develop an automatic flow and/or pressure control system for the equipment presented in Section 2, in the near future. The control strategy is based on directly controlling the torque applied to the induction motor (Nash, 1997).

This paper is organized as follows. In Section 2 the hydraulic test bench together with its main subsystens is presented. In Section 3, white-box and black-box models for the system are developed. Finally, in Section 4, the models performances are compared and final considerations are made about the obtained results.

2 THE HYDRAULIC TEST BENCH

The system studied in this paper is a hydraulic test bench used to analyse the dynamical and static characteristics of hydraulic equipments (Barbosa, 2006). The hydraulic test bench is comprised by two centrifugal pumps connected to 7.5 kW induction motors driven by VFDs, and a hydraulic circuit that allows the implementation of series, parallel, or single pump configurations. The single pump configuration was used to obtain the results presented in the next sections.

In Fig.1 it is shown an overview of the system and its corresponding Pumping and Instrumentation Diagram (P&ID). The optional variable hydraulic load is represented as a dashed circle at the end of the main pipe. This hydraulic load represents any equipment under test.

It is important to note that the speed transmitter indicated in the diagram was used only to identify the motor parameters and to validate the models presented in Section 3, and it is not employed during system normal operation.

The optional hydraulic load was simulated, in the present work, by means of a motorized flow valve at the end of the main pipe. This valve was half opened such that 19.2 l/s flows when the pump operates in nominal speed ($58.3\pi\,\mathrm{rad/s}$).

(a) (b)

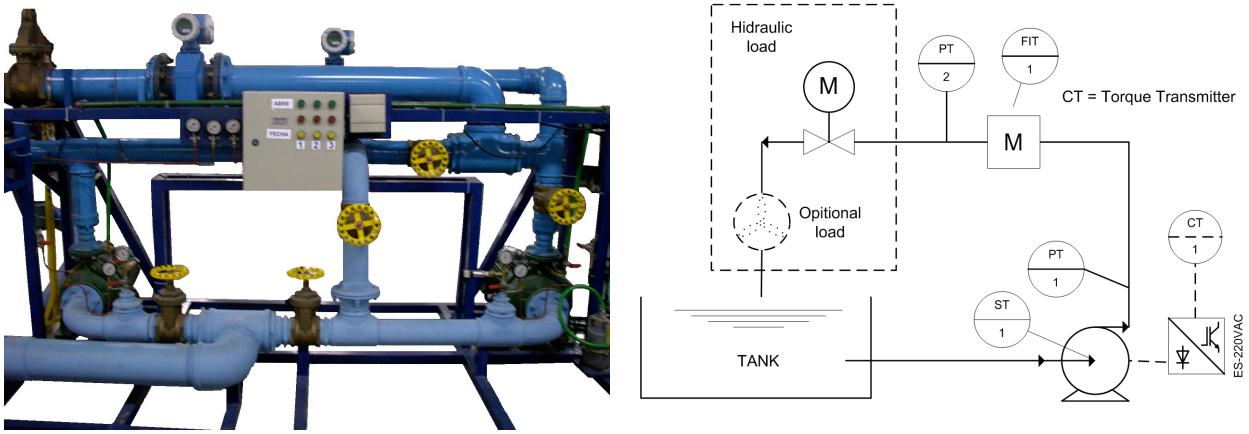

Figure 1. (a) Hydraulic test bench; and (b) the corresponding P&ID diagram.

3 MATHEMATICAL MODELLING

The modelling of real systems can be categorized (Sjöberg et al., 1995) as: (*i*)white-box modeling, when the model is obtained based on physical equations, and a deeper knowledge of the system is usually required; (*ii*) grey-box modeling, when some prior knowledge about the system is used in the identification process; and (*iii*) black-box modeling, when the system is identified based only on experimental time series acquired from the process, without the use of prior knowledge.

In the present work a neural NARMAX black box model (Norgaard, 1997) is presented. This particular model representation and structure has lead to better results than other alternatives, as presented in Barbosa (2006).

A white-box model is also derived from first principles, and its parameters are estimated based on real data acquired during specific tests on the hydraulic bench.

3.1 Black-box model

One important point that deserves consideration during the black–box identification process is the adequate selection of input signals – in this paper the input to the model is the torque reference, which is expressed as a percentage of the motor nominal torque. According to Aguirre (2004) this selection depends on how and where the system will be excited, and also on the available sampling rate.

Considering that the hydraulic pumping system has a variable time-constant (Barbosa et al., 2006) and a non-linear static behavior, the input signal must excite the system around different operating points or equilibrium conditions. The input signal was implemented to excite the process from 5% to 85% of nominal torque of the induction motor through the use of pulses of uncorrelated amplitudes. The pump's speed reaches about 11.7π rad/s and 58.3π rad/s with these torque values.

Fig.2a shows some samples of the input signal. In the identification problem, the auto-covariance of the excitation signal must be similar to the auto-covariance of white noise, as can be seen in Fig.2b. Moreover, the torque amplitudes were obtained from an uniform probability distribution.

The last step to define the input signal is the selection of the sampling time T_s. To adequately choose T_s it must be taken into consideration the auto-covariance of the output signal, which may be either the pressure or the flow produced by the pumping system for a given input reference torque.

Considering that the model output is the system flow, it is necessary to choose a sampling time of at least 100ms since this is the minimum flow transmitter stabilization time observed in a series of tests. For the pressure transmitter, a sampling rate of 1kHz is feasible (Barbosa, 2006), thus a minimum sampling time of 1ms would be possible.

Making use of the aforementioned input signal (Fig.2), with different sampling times, and applying it to the pumping system, adequate T_s were 50ms and 100ms for the pressure and flow system outputs, respectively, according to the analysis of the auto-covariance of the output signals shown in Fig.3. As it can be seen, these sampling times seems to be reasonable for system identification, since the first minimum of each auto-covariance curve is near the recommended interval from 5 to 25 lags (Aguirre, 2004).

Once the input signal was determined and the output data were acquired, the next step to model identification is to define a model structure. Neural NARMAX models were implemented for both pressure and flow system outputs, using a feed-forward multilayer perceptron implemented and described by Norgaard (1997). It was used the function *nnarmax2.m* and the Leverberg-Marquardt algorithm available in the Norgaard toolbox.

The neural network implemented to identify the relation between the torque reference and the pressure output of the

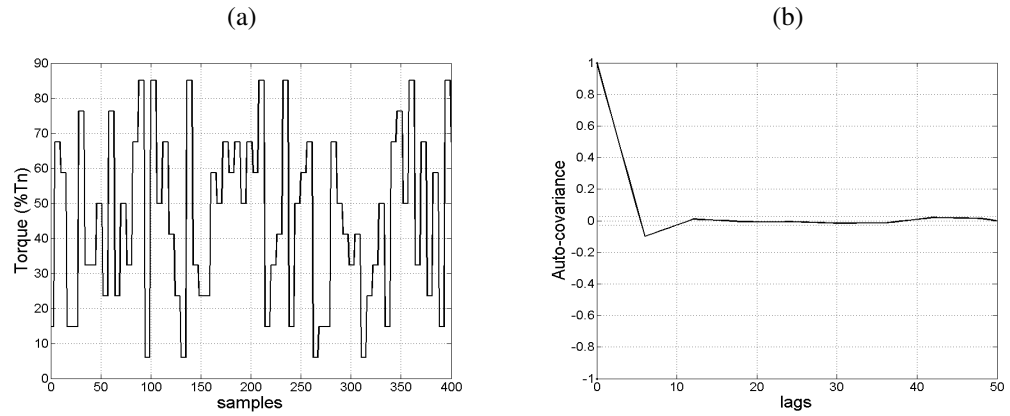

Figure 2. Input signal (torque reference in percent of nominal torque) – (a) samples, (b) auto-covariance.

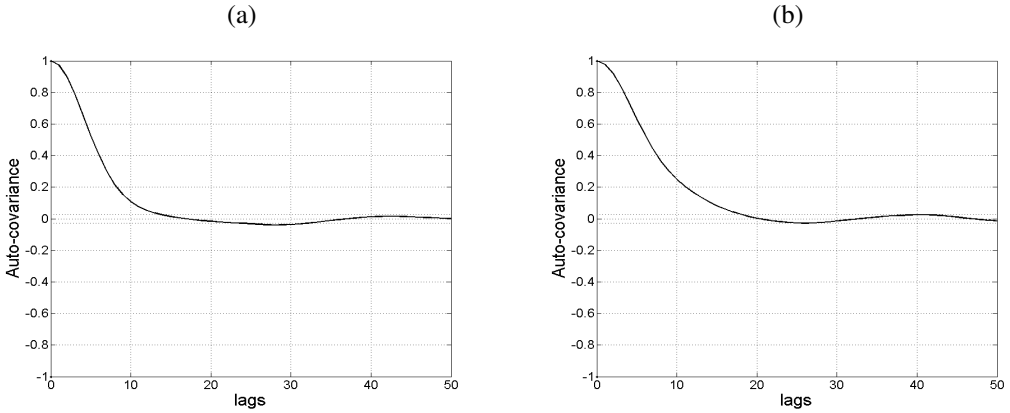

Figure 3. Output signals. (a) Pressure signal auto-covariance, and (b) flow signal auto-covariance.

pumping system has the following features: 12 inputs, where 6 of them are regressive terms of the excitation signal and the others are the regressive terms of the output signal (pressure); 7 non-linear nodes in the hidden layer with hyperbolic tangent activation function and 1 linear node in the output layer. Moreover, a 40 epochs were used to adjust the network weights.

The neural network used to identify the pumping system flow rate has the following features: 14 inputs, where 7 of them are regressive terms of the excitation signal and the others are the regressive terms of the output signal (flow rate); 6 non-linear nodes in the hidden layer with hyperbolic tangent activation function and one linear node in the output layer. 40 epochs were used to adjust the network weights.

The identified models were simulated using only the acquired reference torque input signal time series; i.e. the past output predictions of the neural networks were continuously fed back to the neural networks inputs. The outcomes were evaluated using both dynamic and static data acquired from the process. Fig.4 (a) and (b) shows the dynamic response of the neural NARMAX pressure model as well as the acquired data. Fig.4 (c) and (d) shows the dynamic response of the neural NARMAX flow model together with the acquired data.

As it can be inferred from Fig.4 and Fig.5, the identified models achieved an acceptable dynamic and static response. However, it is necessary to quantify the models performance. In order to accomplish this, the Mean Absolute Percentage Error – MAPE was used, and it can be mathematically expressed as

$$\text{MAPE}_\text{d} = \frac{1}{N}\sum_{k=1}^{N}\frac{|y^*(k) - y(k)|}{y^*(k)}, \tag{1}$$

where N is the number of predicted samples, y^* is the measurement, and y is the model output. The MAPE index used to evaluate the steady-state behavior of the identified model can be readily obtained as

$$\text{MAPE}_\text{s} = \frac{1}{N}\sum_{k=1}^{N}\frac{|\overline{y}_t^* - \overline{y}_t|}{\overline{y}_t^*}, \tag{2}$$

where N is the number of points acquired in steady-state, $\overline{y}_n^*$ is the steady-state measurement corresponding to a specific reference torque input; and $\overline{y}_t$ is the steady-state output of the model.

Using the aforementioned indexes to quantify the quality of the identified models, the neural NARMAX pressure model attained 1.22% and 7.67% for the dynamic and static responses, respectively, and the neural NARMAX flow model achieved 1.10% and 2.60% for the dynamic and static responses, respectively.

The MAPE index corresponding to the steady-state response of the neural NARMAX pressure model was severely affected by the error in the first point of the static characteristic curve (Fig.5a), due to the low pressure value together with its use at the denominator of the expression in the equation (2). Thus, if this point is not considered, the index $MAPE_s$ becomes 1.38%. Both models produced the worst $MAPE_s$ in the low reference input torque situation due to the absence of information corresponding to low torque levels in the excitation signal used during the neural network training process.

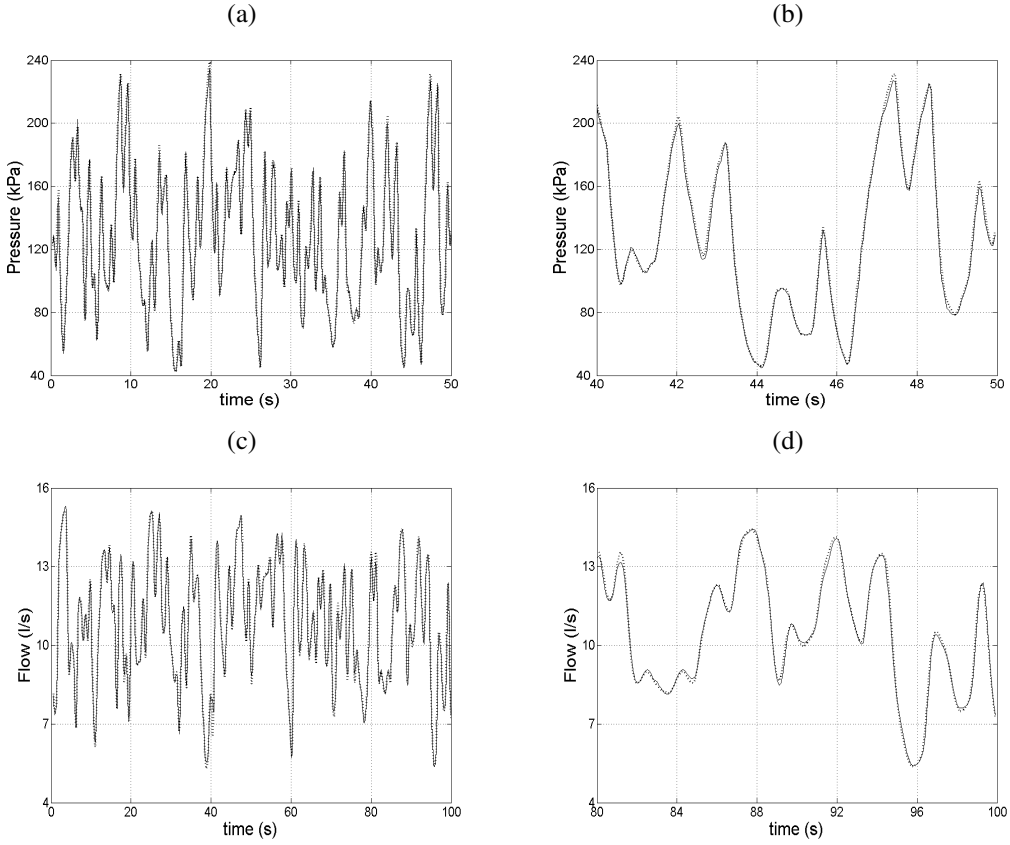

Figure 4. Black-box model validation. (a) Neural NARMAX pressure model validation, and (b) detail of the neural NARMAX pressure model validation. (c) Neural NARMAX model validation for system flow, and (d) detail of the neural NARMAX flow model validation. Solid lines represent the measurement and the dotted ones represent model response.

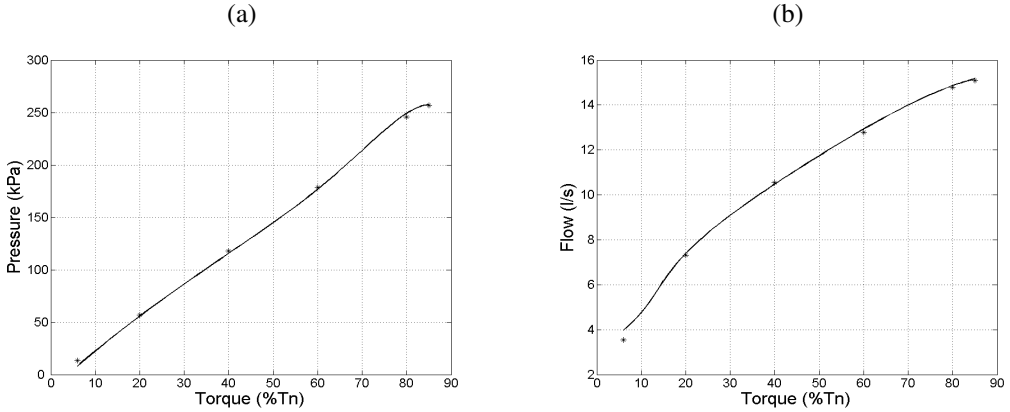

Figure 5. Black-box steady-state model validation. (a) Pressure model static behavior, (b) flow model static behavior. ($*$) denotes the real static data, and the solid line represents the model static response.

3.2 White-box model

The hydraulic test bench can be subdivided into four subsystems: (*i*) Induction motor and variable speed drive; (*ii*) centrifugal pump; (*iii*) fixed hydraulic subsystem, and (*iv*) variable optional hydraulic load. These subsystems are interconnected as depicted in Fig.6.

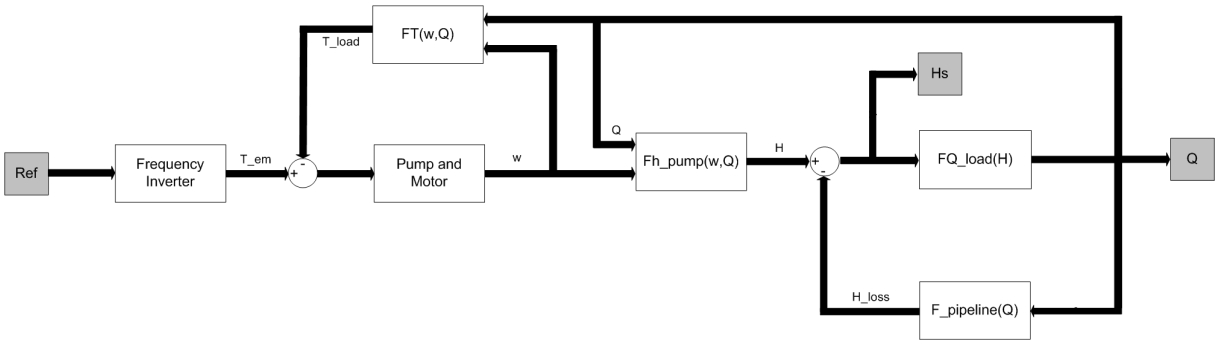

Figure 6. White-box model signal flow diagram. Q is the flow rate and H_s is the pressure at the output of the hydraulic test bench. The functions $F_{\mathrm{H_{pump}}}$, F_T, F_pipeline and FQ_load are static relations obtained in steady-state conditions.

a Induction motor and variable speed drive

Modern vector control techniques allow the direct control of the torque produced by an induction motor, even without speed measurement (Nash, 1997). Using these techniques, from the pressure and/or flow controller point of view, the VFD dynamic response to changes in the reference input torque can be neglected since it is much faster than the desired water pressure and flow variations in the system. Therefore, the combination of VFD together with the induction motor becomes, indeed, an effective torque actuator subsystem, which is used to direct drive the pump in the hydraulic system. The overall behavior is quite similar to that observed if a DC motor, with electrical current control (torque control), was used in place of the induction machine.

Consequently, only the dynamics associated to the mechanical part of the motor and pump needs to be taken into consideration when building the white-box model. We can write the dynamic equation that represent the motor and pump mechanical system as follows:

$$J\frac{d\omega}{dt} = T_\mathrm{e} - b\omega - T_\mathrm{c}\,\mathrm{sgn}(\omega) - F_\mathrm{load}\,(\omega, Q)\,, \tag{3}$$

where ω is the angular speed; Q is the flow produced by the pump; J is the motor and centrifugal pump equivalent moment of inertia; T_e is the electromagnetic torque imposed by the VFD, and whose nominal value is $39.9\,\mathrm{Nm}$; $T_\mathrm{c}\,\mathrm{sgn}(\omega)$ is the Coulomb friction force; b is the viscous friction coefficient; and $F_\mathrm{load}\,(\omega, Q)$ is the opposing hydraulic torque. The parameters in (3) were determined from manufacturers data sheets, and from specific acceleration and deceleration tests: $T_\mathrm{c} = (0.43 \pm 0.02)\,\mathrm{Nm}$, $b = (0.0121 \pm 0.0005)\,\mathrm{Nm/rad/s}$, and $J = 0.08872\,\mathrm{kg\,m^2}$.

The relative absence of relevant dynamics in the production of desired torque values, which is accomplished by the VFD, was confirmed experimentally. Despite this, a static nonlinear relation between the desired torque and the torque effectively produced was observed from experimental data, such that:

$$T_\mathrm{e}\,(u) = \gamma_1 u^5 + \gamma_2 u^4 + \gamma_3 u^3 + \gamma_4 u^2 + \gamma_5 u + \gamma_6, \tag{4}$$

where u is the reference input torque to the VFD, and T_e is the torque effectively produced. The coefficients γ_i, $i = 1, 2, \ldots, 6$, are such that the observed nonlinearity is very small: $\gamma_1 = -1.506 \times 10^{-8}$, $\gamma_2 = 3.843 \times 10^{-6}$, $\gamma_3 = -3.319 \times 10^{-4}$, $\gamma_4 = 1.263 \times 10^{-2}$, $\gamma_5 = 0.707$ and $\gamma_6 = 2.244$.

b Centrifugal pump

The centrifugal pump is used to build up the pressure difference that induces the circulation of water (Driedger, 1995). This pressure difference can be modelled as a static relation depending on pump speed ω and resultant flow rate Q, such that

$$F_{\mathrm{H_{pump}}}\,(\omega, Q) = \alpha_1 Q^3 + \alpha_2 \omega^3 + \alpha_3 Q^2\omega + \alpha_4 Q\omega^2 + \alpha_5 Q^2 + \alpha_6 \omega^2 + \alpha_7 Q\omega + \alpha_8 Q + \alpha_9 \omega + \alpha_{10} \tag{5}$$

where the coefficients α_j, $j = 1, 2, \ldots, 10$, can be estimated from least squares curve fit applied to steady-state values measured during the operation of the hydraulic test bench: $\alpha_1 = -1.3631 \times 10^{-3}$, $\alpha_2 = 1.3620 \times 10^{-9}$, $\alpha_3 = 1.7304 \times 10^{-5}$, $\alpha_4 = -7.3548 \times 10^{-8}$, $\alpha_5 = -2.5497 \times 10^{-2}$, $\alpha_6 = 5.7314 \times 10^{-6}$, $\alpha_7 = 1.0691 \times 10^{-4}$, $\alpha_8 = -9.6703 \times 10^{-2}$, $\alpha_9 = 4.4057 \times 10^{-3}$ e $\alpha_{10} = -2.5259 \times 10^{-1}$.

Similarly, the opposing hydraulic torque, which is demanded in order to drive the pump during normal operation, can also be modelled as a static relation between pump speed ω and resultant flow rate Q. By limiting the polynomial order of this relation to 3, and applying a least squares curve fitting to the steady-state data from the hydraulic test bench system, the following relation was obtained:

$$F_{\mathrm{T}}(\omega, Q) = \beta_1 Q^3 + \beta_2 \omega^3 + \beta_3 Q^2 \omega + \beta_4 Q \omega^2 + \beta_5 Q^2 + \beta_6 \omega^2 + \beta_7 Q \omega + \beta_8 Q + \beta_9 \omega + \beta_{10} \tag{6}$$

where $\beta_1 = -2.5186 \times 10^{-3}$ $\beta_2 = -9.1168 \times 10^{-10}$, $\beta_3 = 6.9103 \times 10^{-5}$, $\beta_4 = 2.5492 \times 10^{-7}$, $\beta_5 = -5.6126 \times 10^{-2}$, $\beta_6 = 1.0972 \times 10^{-5}$, $\beta_7 = 6.8286 \times 10^{-4}$, $\beta_8 = 6.5038 \times 10^{-1}$, $\beta_9 = 3.6776 \times 10^{-3}$ and $\beta_{10} = 4.3067 \times 10^{-1}$. It is important to note that the steady-state values of F_{rmT} were evaluated by means of the estimated torque values indicated by the VFD. Therefore, the mechanical Coulomb and viscous friction forces are also accounted for in the above expression, such that, by combining expressions (3) and (6), one has that $F_{\mathrm{T}}(\omega, Q) = b\omega + T_{\mathrm{c}} + F_{load}(\omega, Q)$, and consequently $\beta_{10} = T_{\mathrm{c}}$.

Although in (Kallesoe et al., 2006) and (Wolfram et al., 2001) lower order polynomials have been adjusted to the steady-state data, it was observed that the white-box model performance is quite sensitive to the correcteness of the static relations (5) and (6), particularly when the ranges of possible speed and flow rates values are increased. In the present case, the MAPE errors were $MAPE_{F_{\mathrm{T}}} = 2.30\%$ and $MAPE_{F_{\mathrm{H_{pump}}}} = 17.01\%$, and the curves were fitted by using data acquired in the ranges $11.7\pi\,\mathrm{rad/s} \leq \omega \leq 58.3\pi\,\mathrm{rad/s}$, and $0\ \mathrm{l/s} \leq Q \leq 27.8\,\mathrm{l/s}$.

c Fixed hydraulic subsystem

The main pipe and associated pipe junctions and elbows on the hydraulic test bench constitutes the fixed hydraulic subsystem. By relying on the general Darcy-Weisbach expression for pressure loss in pipes, which depends on the pipe diameter, length and equivalent friction coefficient (Neves, 1982), it was possible to approximate the pressure loss in the fixed hydraulic subsystem as

$$F_{\mathrm{pipeline}}(Q) \approx k_1 Q^2, \tag{7}$$

where $k_1 = 2.5 \times 10^{-2}$.

d Optional variable hydraulic load

Since the main purpose of the hydraulic test bench is to test diverse hydraulic systems connected at the end of the main pipe, the optional variable hydraulic load is, indeed, an uncertain load that will have to be accounted for in the future control design. In the present study, this uncertain load was mimic by half opening a motorized flow valve at the end of the main pipe in the hydraulic test bench, such that $Q = 19.2\,\mathrm{l/s}$ when $\omega = 58.3\pi\,\mathrm{rad/s}$ (pump nominal speed).

Similarly to what was done for the fixed hydraulic subsystem, by following the Darcy-Weisbach approach, the uncertain hydraulic load can be modelled as producing a pressure loss proportional to the square of the flow rate. The added c constant is due to level difference between the transmitter and the tank, thus

$$FQ_{\mathrm{load}}(H_s) = \frac{\sqrt{H_s + c}}{k_2} \tag{8}$$

where FQ_{load} is the flow rate through the variable hydraulic load; H_s is the corresponding pressure difference; c and k_2 were found to be $c = 0.252$ and $k_2 = 1.082 \times 10^{-1}$ in operational condition described above.

In Fig.7 the white-box model dynamical response is depicted, considering the application of the same reference input torque used to identify the black-box model. The MAPE error was found to be 10.47% for the pressure signal and 3.5% for the flow rate signal. The corresponding static relation obtained from the white-box model is shown in Fig.8 for both pressure and flow rate signals, with MAPE errors of 4.5% and 4.75%, respectively.

4 MODELS COMPARISON AND CONCLUSIONS

From the analysis of the results presented in the previous sections one can conclude that the black-box model performance was superior to the white-box alternative, with respect to the prediction capacity for both pressure and flow rate signals. Table 1 summarizes the MAPE errors found for both models.

An important observation is that the difficulty in obtaining the black-box model was considerably smaller than that registered in the white-box model identification process. This was observed mainly because, in the latter case, a great

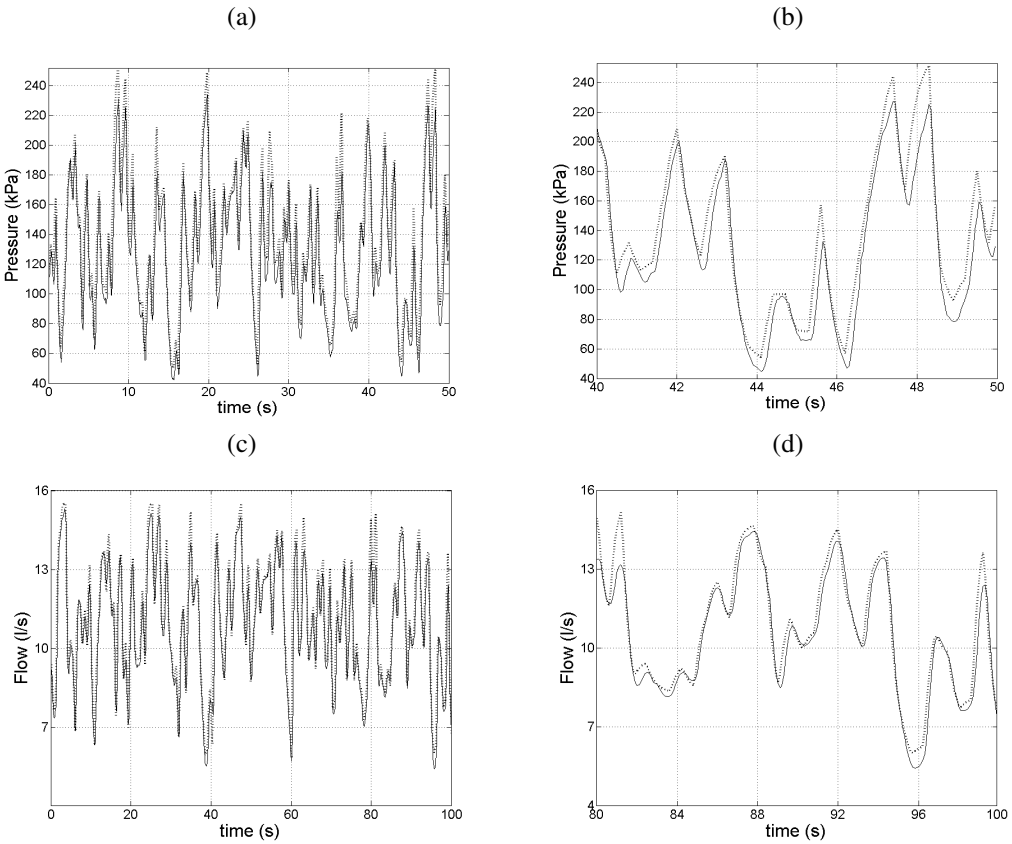

Figure 7. White-box model validation. (a) Pressure model validation, and (b) detail of pressure model validation. (c) Model validation for system flow, and (d) detail of the model validation for system flow. Solid lines represent the measurement and the dotted ones represent the model response.

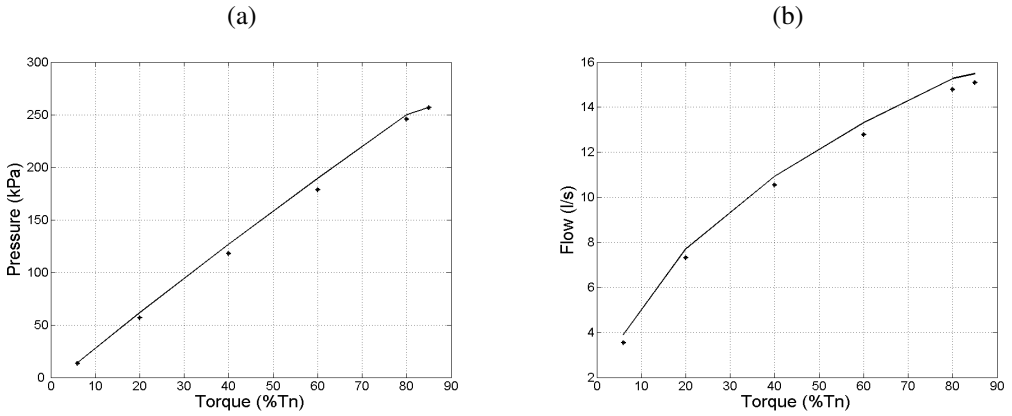

Figure 8. White-box steady-state model validation. (a) Static behavior obtained from the pressure model, and (b) static behavior obtained from the flow model. $(*)$ denotes the real steady-state data, and the solid line represents the corresponding predicted steady-state.

amount of physical insight was demanded in order to adequately represent the hydraulic test bench, and a lot of additional tests were necessary to estimate physically meaningful parameters.

On the other hand, it is also important to note that the black-box model is valid only for the operational condition corresponding to the half opened motorized valve as the optional variable hydraulic load. The same is true for the white-box model, but it has the advantage that it becomes clear how and where the model has to be modified in order to approximate different operational conditions, namely, by adjusting the coefficient k_2 in (8).

Another white-box model advantage is the availability of many other signals in the system, like pump output pressure, pipeline pressure loss and motor speed, through the integration of a simple first order differential equation. Even if the dynamics associated to the water inertial acceleration, caused by the applied pressure difference, was included in the model, as it was done by Eker and Kara (2003), the whole system would still be described by a simple second order

differential equation.

Table 1. White-box and black-box models comparison by means of MAPE indexes.

	Pressure		Flow	
	Static curve	Dynamical response	Static curve	Dynamical response
Black-box model	7.67 / 1.38 %	1.22 %	2.60 %	1.10 %
White-box model	4.50 %	10.47%	4.75 %	3.5%

As a final remark, it is important to highlight that the choice of either model is application dependent. In the present case, since the future objective is the development of control algorithms to track desired pressure or flow rate reference signals, despite the absence of knowledge concerning the uncertain hydraulic load connected to the hydraulic test bench output, the white-box model will be very helpful to predict different behaviors in other operational conditions corresponding to diverse hydraulic loads.

5 REFERENCES

Aguirre, L.A., Introdução à Identificação de Sistemas - Técnicas Lineares e Não-Lineares Aplicadas a Sistemas Reais, Editora UFMG, 2004, 2nd ed.

Barbosa, B.H., 2006, "Instrumentação, Modelagem, Controle e Supervisão de um Sistema de Bombeamento de Água e Módulo Turbina-Gerador," Master's thesis, Universidade Federal de Minas Gerais. Programa de Pós-Graduação em Engenharia Elétrica.

Barbosa, B.H., Aguirre, L.A. and Martinez, C.B., 2006, "Modelos narmax neurais na identificação de um sistema de bombeamento de água," XVI Brazilian Automation Conference, pages 875–880.

Carlson, R., 2000, "Correct method of calculating energy savings to justify adjustable-frequency drives on pumps," IEEE Transactions on Industry Applications, vol. 36, no. 6, pp. 1725 – 1733.

Driedger, W., 1995, "Controlling centrifugal pumps," Hydrocarbon Processing, vol. 74, no. 7, p. 43.

Eker, I. and Kara, T., 2003, "Operation and control of a water supply system," ISA Transactions, vol. 42, no. 3, pp. 461 – 473.

Guevara, Y. and Carmona, R., 1990, "Unsteady and steady flow control on pumping systems," IEEE Transactions on Industry Applications, vol. 26, no. 5, pp. 954 – 960.

Irvine, G. and Gibson, I.H., 2002, "Vf drives: As final control elements in the petroleum industry," IEEE Industry Applications Magazine, vol. 8, no. 4, pp. 51 – 60.

Kallesoe, C.S., Cocquempot, V. and Izadi-Zamanabadi, R., 2006, "Model based fault detection in a centrifugal pump application," IEEE Transactions on Control Systems Technology, vol. 14, no. 2, pp. 204 – 215.

Nash, J.N., 1997, "Direct torque control, induction motor vector control without an encoder," IEEE Transactions on Industry Applications, vol. 33, no. 2, pp. 333 – 341.

Neves, E.T., Curso de Hidráulica, Editora Globo, 1982, sétima ed.

Norgaard, M., 1997, "Neural network based system identification - toolbox," Technical report 97-E-851, Technical University of Denmark.

Pemberton, M., 2005, "Variable speed pumping: Myths and legends," World Pumps, , no. 460, pp. 22 – 24.

Sjöberg, J., Zhang, Q. et al., 1995, "Non-linear black-box modeling in system identification: A unified overview," Automática, pp. 31–1961.

Wolfram, A., Fussel, D. et al., 2001, "Component-based multi-model approach for fault detection and diagnosis of a centrifugal pump," Proceedings of the American Control Conference, vol. 6, pp. 4443 – 4448.

6 Responsibility notice

The authors are the only responsible for the printed material included in this paper